Simulations of Kobe case and Osaka case by the empirical Green's function method considering nonlinear behavior of surface ground

I. Suetomi
Engineering Research Institute, Sato Kogyo Co., Ltd., Tokyo, Japan

N. Yoshida
Engineering Research Institute, Sato Kogyo Co., Ltd., Tokyo, Japan

ABSTRACT: We simulated strong motions in the Kobe area by 1-D equivalent linear analysis using the strong motion records at KBU as the input motion and those in the Osaka area by the empirical Green's function method and 1-D equivalent linear analysis using the aftershock records. It is shown that the nonlinear behavior is significant in soil deposits in the Kobe area and west side of the Uemachi fault in the Osaka area.

1 INTRODUCTION

If there are adequate observation records during small earthquakes, the empirical Green's function method (EGF method: Irikura, 1986) is very useful to simulate strong ground motions because high frequency components is well reproduced as well as low frequency component. Another advantage of this method is that several complicated effects such as the generation and the propagation of surface waves due to the irregularity of the base layer is automatically considered without conducting 2 or 3-D numerical calculations. Kamae & Irikura (1997) showed that this method gives time histories that agrees with observed records during the 1995 Hyogo-ken Nanbu earthquake.

This method, however, seems to have shortage in reproducing the earthquake motion within 20 km from the fault where nonlinear behavior will be predominant because it assumes linear soil behavior. In order to improve this shortage, we propose three steps analytical procedure. At first stage, we apply the empirical Green's function method. Then, we deconvolute the simulated wave to the base layer where nonlinear behavior of soil is small or negligible based on the elastic multi-reflection theory. Finally, earthquake motion at the ground surface is computed by one-dimensional equivalent linear analysis in which computed incident wave in step 2 is used for input.

Figure 1 shows observation sites and the fault. Above mentioned procedure is applicable in the Osaka case because aftershock observation records are given at 4 sites. However, no aftershock observation record is given at KB1, KB2, KB3 and KB4 sites in the Kobe case: only ground conditions

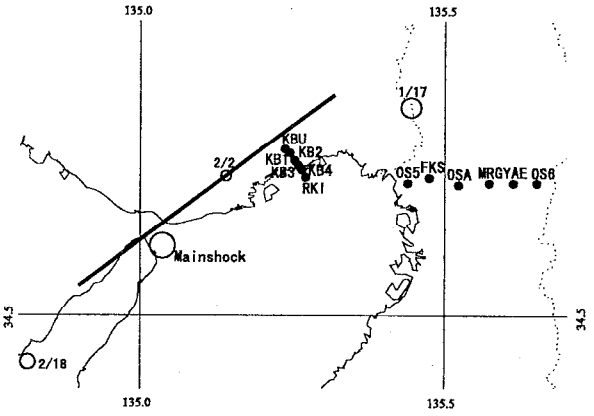

Figure 1. Map of observation sites and the fault.

are given. Nevertheless the records of the mainshock were not observed at these sites, we cannot discuss the accuracy of the proposed method in detail. Alternately, we estimate ground motions using the mainshock record observed at KBU in the Kobe case and focus on the differences of ground motion depending on ground condition.

2 SIMULATION OF KOBE CASE

We estimate ground motions by 1-D equivalent linear analysis (Schnabel et al., 1972) using mainshock records observed at KBU.

2.1 *Incident wave at the base layer*

The observed record at KBU was affected by the nonlinear behavior of the surface deposit, but was not affected so much by the existence of tunnel and the irregularity due to the valley geometry (Suetomi &

Toki, 1997). The incident wave at the base layer is computed by SHAKE using soil profiles shown in Table 1 that is compiled from Iwasaki et al. (1995) and Miyakoshi et al. (1997). Evaluated acceleration time history is shown in Figure 2.

2.2 *Modeling of site conditions*

Shear wave velocity obtained by PS-logging is reported at RKI (Sekisui House, 1996). As shear wave velocity is not given at other sites, we evaluate shear wave velocity from the average SPT N-value in each layer by using the empirical formula (Japan Road Association, 1990):

Table 1. Soil profile model at KBU

No.	Soil type	Thickness (m)	Density (t/m^3)	V_S (m/s)
1	surface soil	6.10	1.90	319
2	silt	5.65	1.80	240
3	weathered granite	4.25	1.97	340
4	weathered granite	4.80	2.27	590
5	weathered granite (D class)	12.20	2.08	850
6	weathered granite (D class)	7.45	2.06	960
7	weathered granite (C_L class)	12.50	2.18	1120
8	weathered granite (C_M class)	67.85	2.2	1350
9	weathered granite	200.0	2.4	1800
10	bedrock	-	2.7	3200

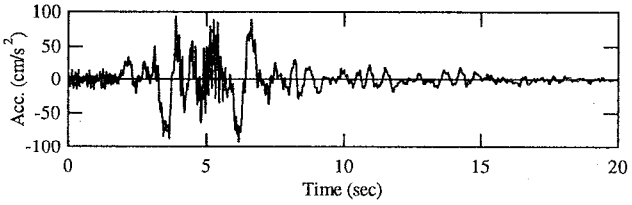

Figure 2. Calculated incident wave (NS comp.) at KBU.

Table 2(a). Soil profile model at KB1

No.	Soil type	Thickness (m)	Density (t/m^3)	V_S (m/s)
1	surface soil	0.50	1.6	190
2	sand	3.80	1.8	270
3	gravel	2.20	1.9	350
4	sand	1.10	1.8	270
5	silty fine sand	0.80	1.8	320
6	sand	12.1	1.8	350
7	upper Osaka Group	80.0	1.8	550
8	lower Osaka Group	400.0	2.1	1000
9	bedrock	-	2.7	3200

Table 2(b). Soil profile model at KB2

No.	Soil type	Thickness (m)	Density (t/m^3)	V_S (m/s)
1	sand	3.00	1.7	280
2	gravel	4.10	1.9	350
3	silt	0.20	1.7	250
4	gravel	12.70	1.9	350
5	upper Osaka Group	280.0	1.8	550
6	lower Osaka Group	560.0	2.1	1000
7	bedrock	-	2.7	3200

Table 2(c). Soil profile model at KB3

No.	Soil type	Thickness (m)	Density (t/m^3)	V_S (m/s)
1	surface soil	6.60	1.6	190
2	sand	3.40	1.8	280
3	silty fine sand	2.50	1.7	220
4	sand	3.00	1.8	320
5	silty fine sand	1.30	1.7	240
6	sand	1.10	1.8	350
7	silt	0.50	1.7	210
8	gravel	48.0	1.7	350
9	upper Osaka group	440.0	1.8	550
10	lower Osaka group	720.0	2.1	1000
11	bedrock	-	2.7	3200

Table 2(d). Soil profile model at KB4

No.	Soil type	Thickness (m)	Density (t/m^3)	V_S (m/s)
1	fill	18.60	1.7	190
2	silt	3.00	1.6	130
3	sand	1.10	1.8	260
4	silt	0.80	1.6	180
5	gravel	8.00	1.8	350
6	silt(Ma13)	10.0	1.6	220
7	gravel	30.0	1.8	350
8	silt(Ma12)	15.0	1.6	270
9	gravel	50.0	1.8	350
10	upper Osaka group	520.0	1.8	550
11	lower Osaka group	830.0	2.1	1000
12	bedrock	-	2.7	3200

Table 2(e). Soil profile model at RKI

No.	Soil type	Thickness (m)	Density (t/m^3)	V_S (m/s)
1	fill	22.50	1.9	360
2	fill	3.00	1.9	250
3	clay(Ma13)	10.00	1.65	200
4	clay(Ma13)	4.50	1.7	220
5	gravel	11.0	1.8	380
6	gravel	24.0	1.9	340
7	silt(Ma12)	20.0	1.6	270
8	gravel	140.0	1.8	350
9	upper Osaka group	640.0	1.8	550
10	lower Osaka group	1000.0	2.1	1000
11	bedrock	-	2.7	3200

$$V_S = 100N^{1/3} \quad \text{(sand)}$$
$$V_S = 80N^{1/3} \quad \text{(clay)} \qquad (1)$$

Deep sedimentary structure estimated by Kagawa et al. (1993) and Miyakoshi et al. (1997) is used.

Strain dependent characteristics of the shear modulus and damping coefficient obtained at Port Island (Kobe City, 1995), Shin-Kobe Service Station (Matsumoto et al., 1996) and Kobe Univ. of Mercantile Marine (Iwata et al., 1996) are used in the analysis. When they are not sufficient, the empirical formula proposed by Yasuda & Yamaguchi (1985) are also used.

2.3 *Results of the simulation*

The calculated acceleration time history at RKI where the mainshock record was observed is compared with the observed record in Figure 3. The calculated waveform is fairy smooth because of the lack of high frequency components, whereas the observed waveform shows a sharp peak. Under the strong ground motion, equivalent linear analysis has a tendency to absorb high frequency component because large damping ratio that corresponds to large effective strain is applied in whole time. The peak in the calculated wave appear earlier than that of the observed wave. Beside it, equivalent linear analysis grasps the general features of the response such as the peak value well. If we use the effective stress analysis, we will be able to get better waveform in the same manner with the case of Port Island (Suetomi & Yoshida, 1998).

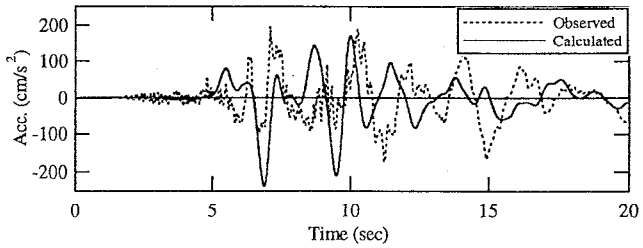

Figure 3. Comparison between calculated and observed acceleration waveforms (NS comp.) at RKI.

Figure 4 shows calculated acceleration time histories at the ground surface at 6 sites. These are arranged following the distance from KBU. It is shown that peak values are larger at KB1 and KB2 than those at other sites, and that waveforms at KB4

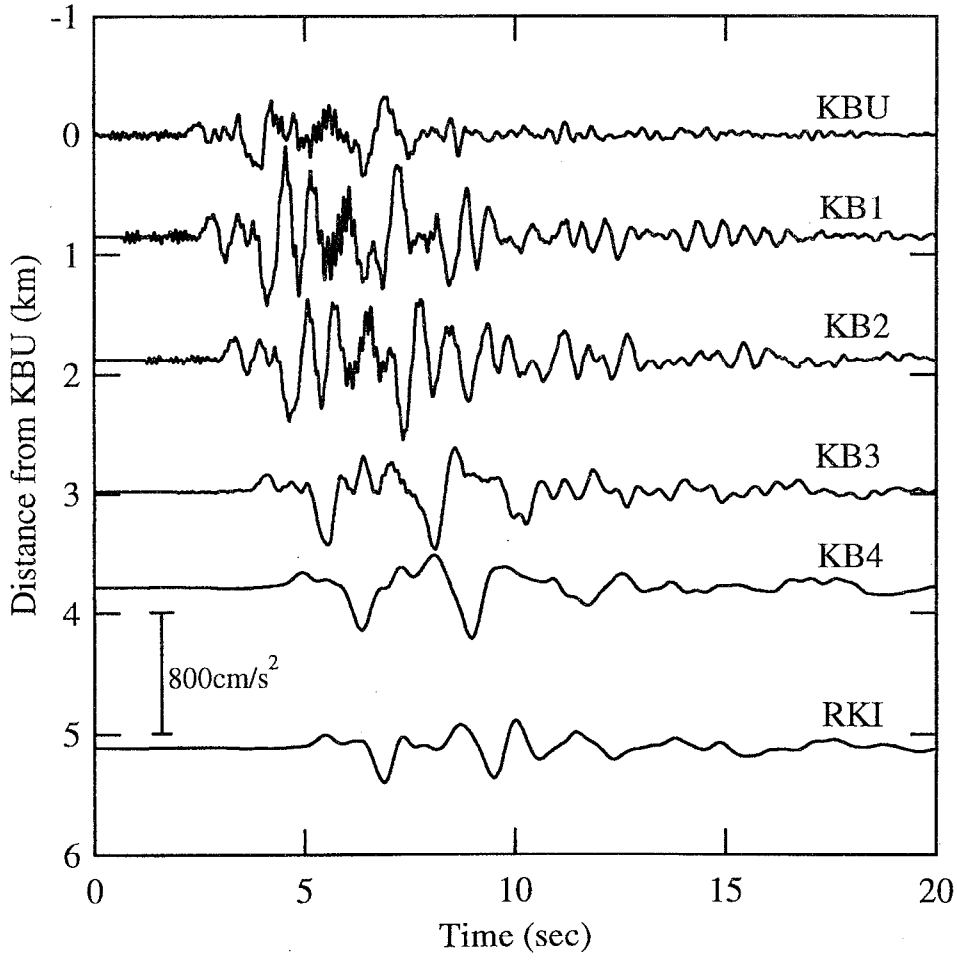

Figure 4. Simulated acceleration waveforms (NS comp.) along the KBU-RKI line.

and RKI that are located close to the sea are very smooth. Figure 5 shows transfer functions at each site. It is shown that amplification ratios in the frequency higher than 1 Hz are very small at KB4 and RKI. Acceleration response spectra (h=5%) are shown in Figure 6 and distributions of calculated peak ground acceleration (PGA), peak ground velocity (PGV) and JMA seismic intensity scale (I_{JMA}) at the ground surface along the KBU-RKI line are shown in Figure 7. As the maximum response from 0.5 to 1.0 seconds are very large at KB1 and KB2, PGA at KB1 and KB2 are larger than other sites. As the maximum response longer than 2 seconds are large at KB3 and KB4, PGVs at KB3 and KB4 are as large as those at KB1 and KB2. PGV at RKI is small because that at the top of Osaka group layer is small. Tokimatsu et al. (1997) shows that the damage belt region can be explained by only 1-D analysis for Higashi-Nada ward. It suggests us that PGV does not always become larger as the base layer becomes deeper.

KB2 is located in the damage belt, but KB1 is not. Nevertheless, peak parameters at KB1 are larger than those at KB2. This is because the alluvial layer at KB1 is more thick and softer than that at KB2. PGV at KB2 will be larger than that at KB1 computed by 2 or 3-D analyses considering deep irregular ground structure, then it can be concluded that the 1-D analysis cannot explain the disaster. We must, however, notice that, although KB1 is not located in the damage belt zone, the damage near the KB1 was not slight. On the contrary, KB2 is located in the damage belt zone but the damage near the KB2 was not severe. This indicates that the relationship between the degrees of damage and index of ground motion such as PGA and PGV is not simple. Therefore, we must discuss the relation between the ground motion and the disaster carefully.

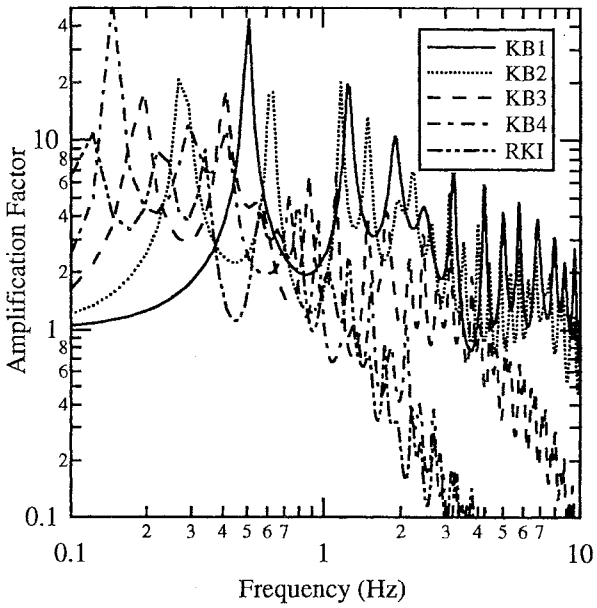

Figure 5. Transfer Functions.

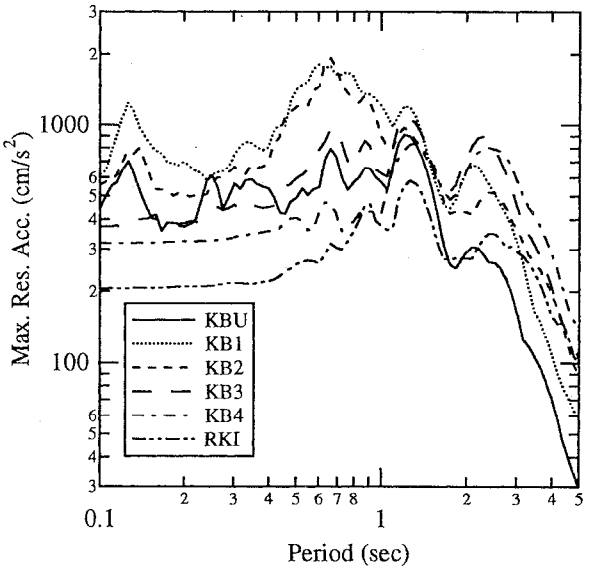

Figure 6. Acceleration response spectra (h=5%).

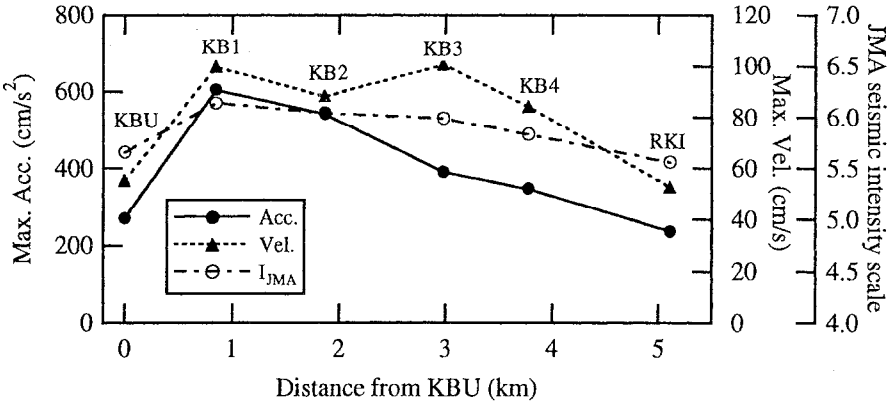

Figure 7. Distribution of PGA, PGV and JMA seismic intensity scale along the KBU-RKI line.

3 SIMULATION OF OSAKA CASE

3.1 *Conditions of empirical Green's function method*

The observation records during the mainshock and aftershock are given at 4 sites in the Osaka case, therefore the EGF method can be adopted for FKS, OSA, MRG and YAE. The incident waves at the layer whose shear wave velocity is 350 m/s are calculated by the 1-D linear analysis. Then ground motions at the ground surface are calculated by the equivalent linear analysis. As earthquake records are not observed at OS5 and OS6, the incident waves at the adjacent observation site (FKS for OS5 and YAE for OS6) are used as the input motion. The difference of deep underground structure, and distance and radiation from the fault are ignored.

The calculation by the EGF method is carried out by dividing the fault into 3 subevents as shown in Figure 8 (Kamae & Irikura, 1997). It is noted, however, aftershock records given in this simulation are not the same with those which are used by them. In this simulation, only one aftershock of February 2 is used for 3 subevents whereas they used 3 aftershock records which reflect source and path effect from each subevent. The slip distribution in each subevent is assumed to be uniform. The fault rupture is assumed to propagate from the hypocenter in a circle. The velocity of the fault rupture is set to be 2.8 km/s. The shear wave velocity of rock is set to be 3.5 km/s. Rise time is set at 0.6 seconds (Kamae & Irikura, 1997). For the simplicity, the dip angle of 3 subevents are set to be 90 degrees.

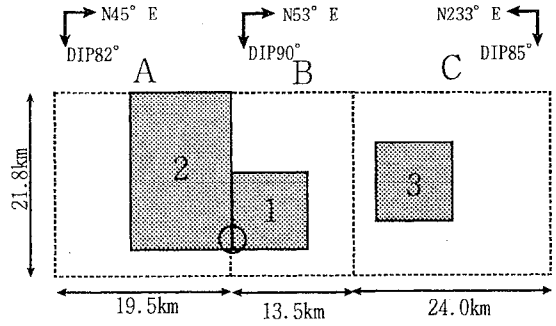

Figure 8. Fault model by Kamae & Irikura (1997).

Table 3(a). Soil profile model at OS5

No.	Soil type	Thickness (m)	Density (t/m^3)	V_S (m/s)
1	surface soil	1.7	1.7	100
2	sand	1.3	1.8	100
3	sand	6.0	1.8	180
4	silt	14.4	1.6	100
5	silty fine sand	3.3	1.7	200
6	gravel	-	1.8	350

Table 3(b). Soil profile model at FKS

No.	Soil type	Thickness (m)	Density (t/m^3)	V_S (m/s)
1	surface soil	1.4	1.6	120
2	sandy silt	1.6	1.7	140
3	sand	1.4	1.7	180
4	sand	1.5	1.8	250
5	sand	1.7	1.7	210
6	silty clay	11.8	1.5	120
7	silt	6.0	1.6	180
8	sand	1.7	1.7	320
9	gravel	-	1.8	350

Table 3(c). Soil profile model at OSA

No.	Soil type	Thickness (m)	Density (t/m^3)	V_S (m/s)
1	surface soil	1.7	1.7	170
2	silty sand	2.7	1.7	160
3	gravel	3.5	1.8	280
4	clay	4.8	1.6	130
5	clay	1.1	1.6	160
6	gravel	6.4	1.8	350
7	silty clay	5.1	1.6	190
8	sand	-	1.8	350

Table 3(d). Soil profile model at MRG

No.	Soil type	Thickness (m)	Density (t/m^3)	V_S (m/s)
1	surface soil	0.3	1.7	100
2	gravel	1.6	1.8	230
3	clay	2.1	1.5	80
4	sand	1.6	1.7	210
5	clay	10.1	1.6	100
6	silt	2.5	1.7	140
7	gravel	-	1.8	350

Table 3(e). Soil profile model at YAE

No.	Soil type	Thickness (m)	Density (t/m^3)	V_S (m/s)
1	surface soil	1.6	1.6	140
2	silt	0.5	1.6	100
3	sand	1.3	1.7	180
4	sand	1.4	1.8	280
5	silt	3.9	1.6	120
6	clay	4.8	1.6	80
7	clay	3.9	1.6	140
8	sand	1.2	1.8	320
9	clay	2.0	1.7	190
10	gravel	-	1.8	350

Table 3(f). Soil profile model at OS6

No.	Soil type	Thickness (m)	Density (t/m^3)	V_S (m/s)
1	surface soil	1.6	1.7	140
2	silt	1.4	1.6	110
3	sand	0.8	1.7	190
4	sand	4.0	1.8	240
5	sand	1.7	1.8	340
6	silt	1.1	1.6	180
7	gravel	-	1.8	350

3.2 *Modeling of site conditions*

Soil profile models upper than the layer whose shear wave velocity is 350 m/s are evaluated by the procedure same with the Kobe case at 6 sites, resulting in Table 3. Strain dependent characteristics of the shear modulus and damping coefficient are estimated from the empirical formula (Yasuda & Yamaguchi, 1985).

3.3 *Results of the simulation*

Figure 9 shows acceleration time histories of the observed wave, the calculated wave by the EGF method, and the calculated wave by both the EGF method and SHAKE at FKS. High frequency component is more predominant in the case when nonlinear effect is not considered than the observed record. The wave considering the nonlinear effect is in good agreement with the observed wave. Figure 10 shows transfer functions by two methods at FKS.

The nonlinear effect is apparently seen at FKS. The peak value before 30 sec is larger than that after 30 sec in the observed wave, but it is smaller than that after 30 sec in the calculated wave. One of the reason is that only one aftershock record is used for the 3 subevents. The component due to the surface wave is overestimated because the aftershock record which occurred at the center of the fault is also used for subevent A (Awajishima side).

Here, we used equivalent linear analysis based on S-wave for the back part in which the surface wave seemed to be predominant. Strictly speaking, the calculated wave by the EGF method should be divided into two parts before the analysis. The nonlinear behavior is, however, also seen in the back part of the observed wave. It is future subject to express the nonlinear behavior by the surface wave.

Figure 11 shows calculated acceleration time histories at the ground surface at 6 sites along the FKS-YAE line. These are arranged following the distance from OS5. The ground motions at OS5 and FKS which are seaside from the Uemachi fault are apparently larger than those at other sites (mountain side). The back parts are especially quite different. Distribution of the calculated PGA and PGV at the ground surface along the FKS-YAE line are shown in Figure 12. PGV shows a similar tendency with PGA unlike Kobe case. PGA and PGV at OSA are the smallest because the seismometer is in the tall building. Such effect is also contained in the EGF method.

4 CONCLUSIONS

The conclusions are as follows:

1) General features of the response are well grasped by the empirical Green's function method.
2) It is shown that the nonlinear behavior of soil deposits is significant in the Kobe case and west side of the Uemachi fault in the Osaka case. Therefore empirical Green's function method must be applied considering the nonlinear behavior of surface ground as proposed in this paper.

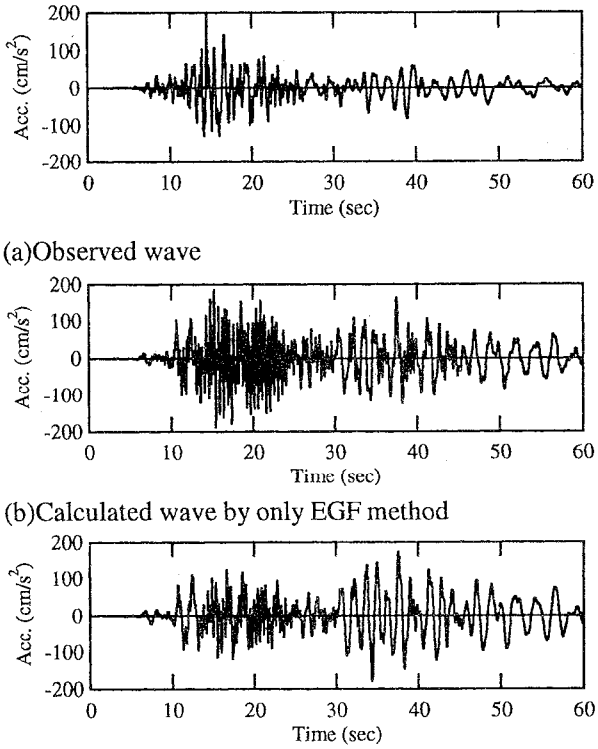

Figure 9. Comparison of time histories (EW comp.) at FKS.

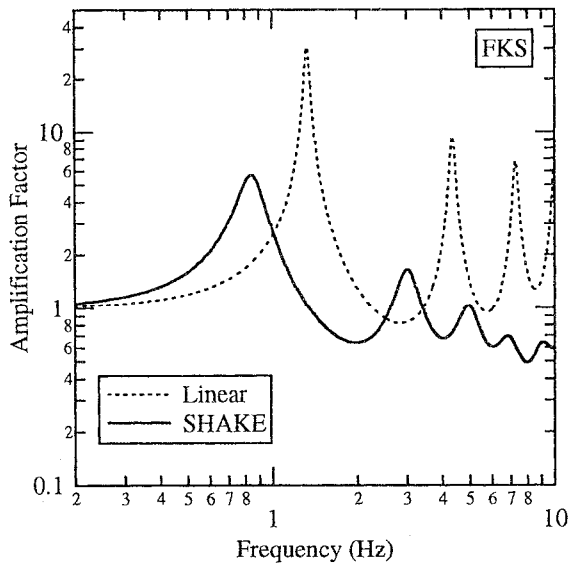

Figure 10. Comparison of transfer functions at FKS.

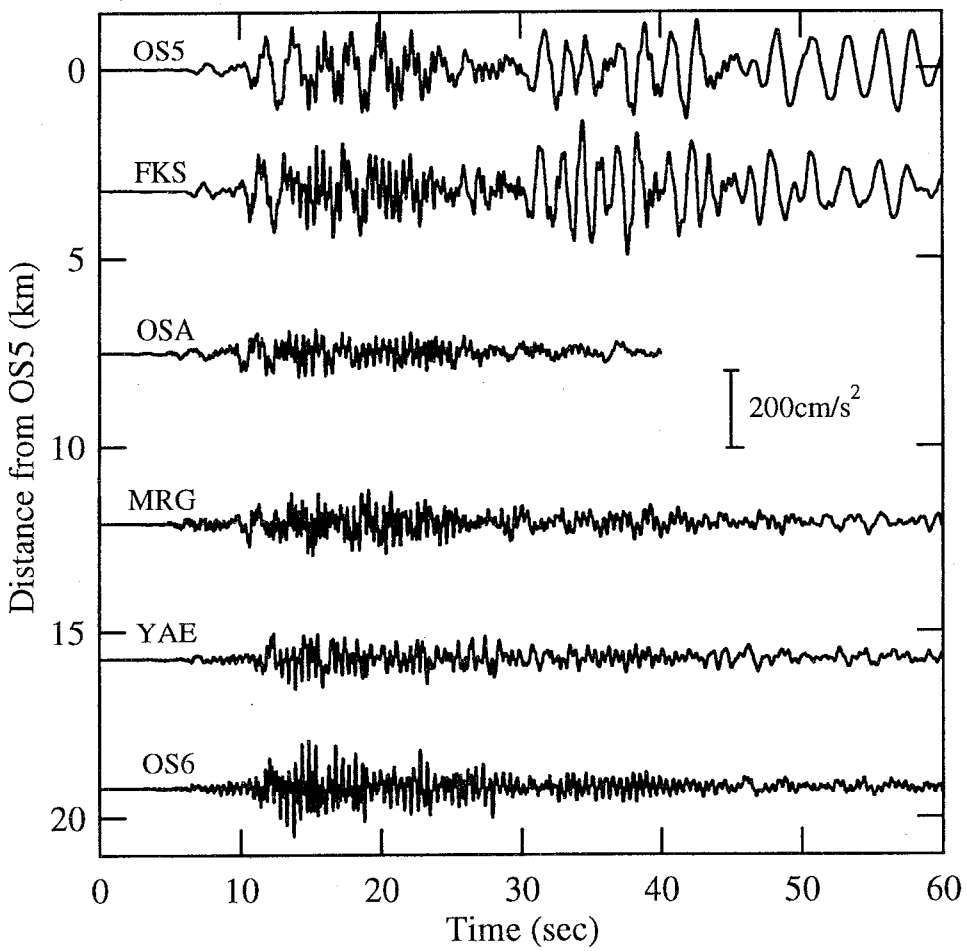

Figure 11. Calculated acceleration time histories (EW comp.) along the FKS-YAE

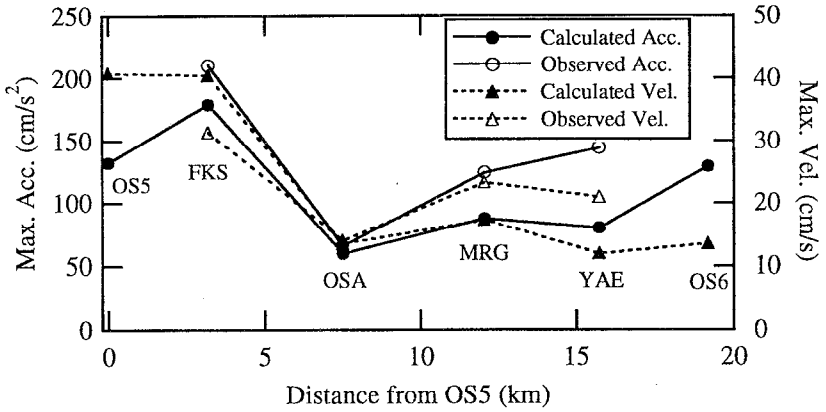

Figure 12. Computed peak ground acceleration (PGA) and peak ground velocity (PGV) along the FKS-YAE line.

ACKOWLEDGEMENTS

The authors would like to express their deep appreciation to the Committee for Earthquake Observation and Research in Kansai Area, Sekisui House and the Japan Meteorogical Agency.

REFERENCES

Irikura, K. 1986. Prediction of strong acceleration motion using empirical Green's function, *Proc. 7th Japan Earthq. Symp.*: 151-156.

Iwasaki, Y., T.Hongo, Y.Yokota & S.Itoh 1995. Ground charactristics of the Rokko-Dai(Kobe Univ.) ground motion monitoring site, *Programme*

and Abstracts, the Seism. Soc. of Japan: **2**, P77 (in Japanese).

Iwata, T. et al. 1996. Geophysical structure in Kobe area, *Grant-in-Aid for Co-operative Research (A) No.07300005, Head Investigator: Fujiwara, T.*:II-21-49 (in Japanese).

Japan Road Association. 1990. *Specifications for Highway Bridges, Part V, Earthquake Resistant Design* (in Japanese).

Kagawa, T., S.Sawada, Y.Iwasaki and A.Nanjo. 1993. Modeling of deep sedimentary structure of the Osaka Basin, *Proc. 22th JSCE Eqrth q. Eng. Symp.*: 199-202 (in Japanese).

Kamae, K. & K.Irikura. 1997. A fault model of the 1995 Hyogo-ken Nanbu earthquake and s imulation of strong ground motion in near-sou rce area, *J. Struct. Constr. Eng., AIJ*: **500**, 29-36.

Kobe City Development Bureau. 1995. *Report of Investigation for Liquefaction-induced Large Ground Displacement at Reclaimed Land (Port Island and Rokko Island)* (in Japanese).

Matsumoto, M., Koike, A. and Y.Sawada 1996. Evaluation of ground motion characteristics of the great Hanshin earthquake in near-field bedrocks, *JSCE Symp. on Hanshin-Awaji Great Earthquakes, JSCE*: 81-84 (in Japanese).

Miyakoshi, K., T.Kagawa and T.Echigo 1997. D eep sedimentary structure model beneath the O saka Plain, *Proc. 96th, SEGJ* (in Japanese).

Schnabel, P.B., J.Lysmer & H.B.Seed 1972. SHAKE a computer program for earthquake response analysis of horizontally layered sites. *EERC*: 72-12.

Sekisui House 1996. *Rokko Island City, 1995 Hyogoken-Nanbu earthquake observation and analysis* (in Japanese).

Suetomi, I. & K.Toki 1997. The effect of surface deposit at Kobe Univ., *Proceedings of the 24th JSCE Earthq. Eng. Symp.*: 57-60 (in Japanese).

Suetomi,I. & N.Yoshida 1998. Nonlinear behavior of surface deposit during the 1995 Hyogoken-Nambu earthquake, *Special issue of Soils and Foundations*: 11-22.

Tokimatsu, K., H.Arai & Y.Asaka 1997. Deep shear-wave structure and earthquake ground motion characteristics in Sumiyoshi area, Kobe city, based on microtremor measurements, *J. Struct. Constr. Eng., AIJ*, **491**: 37-45 (in Japanese).

Yasuda, S. & Yamaguchi, I 1985. Dynamic shear modules obtained in the laboratory and in-situ, *Proc. Symp. on Evaluation of Deformation and Strength of Sandy Grounds, JMSMFE:* 115-118 (in Japanese).

ESG 1998

Second International Symposium on The Effect of Surface Geology on Seismic Motion

-Recent Progress and New Horizon on ESG Study-

Special Volume on Simultaneous Simulation for Kobe

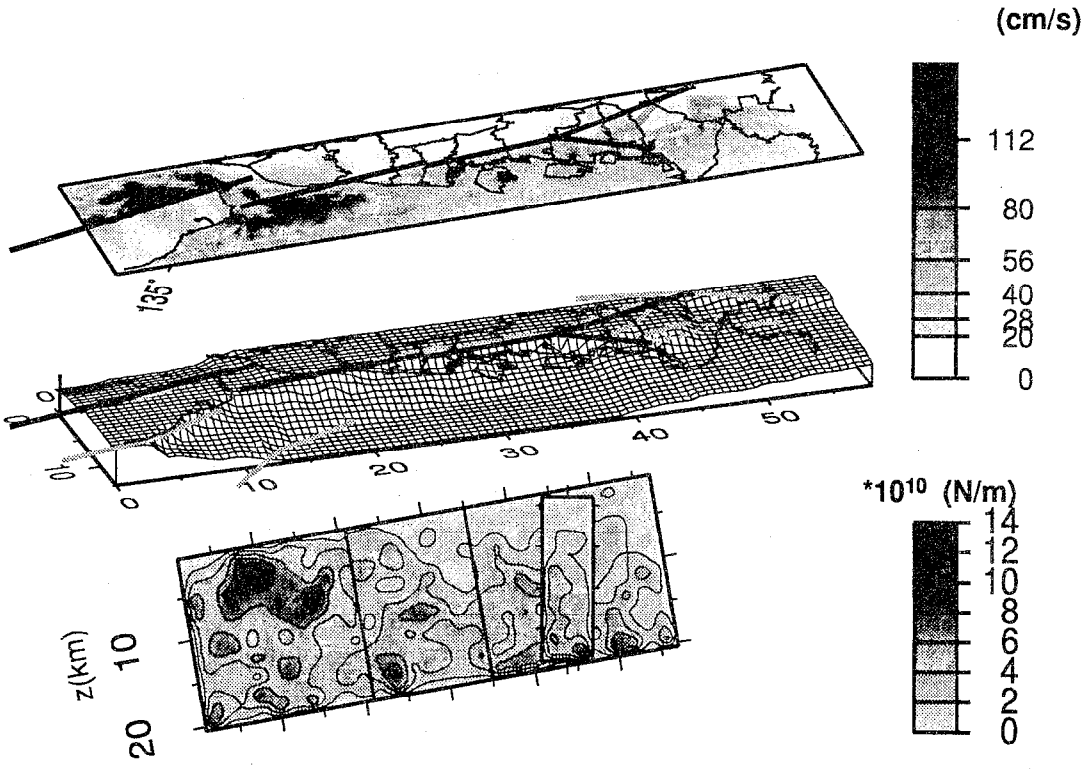

Local Organizing Committee for the 2nd International Symposium on the Effects of Surface Geology on Seismic Motion